



1 **Juniper tree-ring data from the Kuramenian Mountains**
2 **(Republic of Tajikistan), reveals changing summer drought**
3 **signals in western Central Asia**

4 Feng Chen¹, Tongwen Zhang¹, Andrea Seim², Shulong Yu¹, Ruiibo Zhang¹, Hans W. Linderholm²
5 , Zainalobudin V. Kobuliev³, Ahsan Ahmadov³, Anvar Kodirov³

6 ¹ Key Laboratory of Tree-ring Physical and Chemical Research of China Meteorological
7 Administration/Xinjiang Laboratory of Tree-Ring Ecology, Institute of Desert Meteorology, China
8 Meteorological Administration, Urumqi 830002, China,

9 ² Regional Climate Group, Department of Earth Science, University of Gothenburg, Gothenburg,
10 Sweden

11 ³ Institute of Water Problems, Hydroenergy and Ecology, Academy of Science of the Republic of
12 Tajikistan, Dushanbe 734063, Tajikistan

13 *Correspondence to:* Feng Chen (feng653@163.com)

14

15 **Abstract.** Coniferous forests cover the mountains in many parts of central Asia and provide large
16 potentials for dendroclimatic studies of past climate variability. However, to date, only a few
17 tree-ring based climate reconstructions exist from this region. Here we present a regional tree-ring
18 chronology from moisture-sensitive *Juniperus seravschanica* from the Kuramenian Mountains
19 (Republic of Tajikistan), which is used to reveal past summer drought variability in western
20 Central Asia. The chronology accounts for 40.5% of the variance of the June–July self-calibrating
21 Palmer Drought Severity Index (scPDSI) during the instrumental period (1901 to 2012). Seven dry
22 periods including 1659–1696, 1705–1722, 1731–1741, 1758–1790, 1800–1842, 1860–1875 and



23 1931–1987, and five wet periods of 1742–1752, 1843–1859, 1876–1913, 1921–1930 and
24 1988–2015 were identified. Good agreements between drought records from western and eastern
25 Central Asia suggest that the PDSI records retain common drought signals and captures the
26 regional dry/wet periods of Central Asia. Moreover, the wavelet analysis indicates the existence of
27 centennial (100-150 years), decadal (50-60, 24.4 and 11.4 years) and interannual (8.0 and 2.0-3.5
28 years) cycles, which may linked with climate forcings, such as solar activity and ENSO. The
29 analysis between the scPDSI reconstruction and large-scale atmospheric circulations during the
30 reconstructed extreme dry and wet years can provide information about the linkages of extremes
31 in our scPDSI record with the Asian summer monsoon activity.

32 **Keywords:** Kuramenian Mountains; Tree rings; Drought reconstruction; Synoptic climatology
33 analysis; Tajikistan; Juniper

34 **1 Introduction**

35 As a result of climate warming during recent decades, the intensity and frequency of drought
36 events have been increasing (Easterling et al., 2000; Dai et al., 2011; Schrier et al., 2013). Climate
37 models predict a significant increase in the extent of dry areas across the globe, mainly in the
38 Northern Hemisphere, with an potential expansion of arid lands by up to 80% in developing
39 countries (Huang et al., 2015). Climate change and related drought events have significant
40 influences on the socioeconomic and human well-being in arid Central Asia, particularly in
41 densely populated dry lands, such as the Fergana Basin (Ososkova et al., 2000; Siegfried et al.,
42 2012; Yao et al., 2015). Lake shrinkage, oasis salinization, and water resource deterioration,
43 mainly due to excess water use for irrigation, have been linked to climate change, especially in the
44 Aral Sea Basin (Micklin, 1988; Lioubimtseva and Cole, 2006; Kezer and Matsuyama, 2006; Reyer



45 et al., 2015). Meteorological stations were installed at some big cities of Central Asia, such as
46 Samarkand, in the late 19th century, but most of observational records from the mountains areas of
47 Central Asia started in the 1950-1960s. Due to poor spatiotemporal coverage of meteorological
48 records in the mountains areas, there are uncertainties in the estimation of Central Asian climate
49 change. Therefore, to achieve more accurate assessments of climate change in a long-term
50 perspective in this region, high-resolution climate proxy data is needed.

51 Due to their exact dating and annual resolution, climate-sensitive trees play an important role
52 in providing information about past climate variability and change in many regions of the world
53 (Jones et al., 2009). Indeed, many of the existing long-term climate records from Central Asia
54 have been based on tree-ring data (Esper et al., 2001, 2002, 2003; Yuan et al., 2003; Chen et al.,
55 2010, 2014; Zhang et al., 2013; Solomina et al., 2014). These dendroclimatic reconstructions
56 allow us to better understand the spatiotemporal variations of Central Asian climate. However, the
57 impact of climate on tree growth can be complex, where for tree-ring formation can be influenced
58 by both precipitation and temperature (Fritts, 1976; Tian et al., 2007), making it difficult to
59 separate the precipitation signals from temperature. However, by considering monthly climate
60 factors and the soil moisture supply, different comprehensive drought indices, such as the
61 standardized precipitation evapotranspiration index (Vicente-Serrano et al., 2010) and the PDSI
62 (Palmer, 1965) and, have been developed. Such indices can thus be used as targets for drought
63 reconstructions from trees with as mixed temperature and precipitation sensitivity. . Based on large
64 tree-ring networks, spatial drought reconstructions have been developed for many regions,
65 including Europe, North America, northwestern Africa and Mongolia (e.g. Cook et al., 1999, 2010,
66 2015; Davi et al., 2010; Fang et al., 2010; Seftigen et al. 2015; Touchan et al., 2011). Although



67 some dendroclimatic studies have investigated drought variability, as well as its effect on tree
68 growth in Central Asia (Esper et al., 2001; Yuan et al., 2003; Chen et al., 2013, 2015a, 2015b,
69 2016; Seim et al., 2015, 2016), the number of tree-ring data from western Central Asia is still not
70 sufficient to provide a regionally comprehensive picture. . To achieve this additional
71 moisture-sensitive tree-ring chronologies are needed.

72 The Kuramenian Mountains offer good potentials for dendroclimatic study in Northern
73 Tajikistan. This mountain range is a source of streamflow into the small mountainous rivers in the
74 border areas between Tajikistan and Uzbekistan. The exploding population and scarce water
75 resources have stressed water supplies increasingly in the Fergana basin and its surrounding areas.
76 Dendroclimatic information from the Kuramenian Mountains can be used to make water resource
77 plans and help tackle regional climate change. This study presents a June–July PDSI
78 reconstruction from tree-ring width data of Turkestan juniper, obtained from two sites in the
79 Kuramenian Mountains, northern Tajikistan. Wavelet analysis were applied to examine any cycles
80 in the drought reconstruction. Furthermore, we investigated relationships between this drought
81 record and the Asian summer monsoon and atmospheric circulation patterns over the Pacific and
82 Indian Oceans.

83 **2 Material and methods**

84 2.1 Geographical settings and chronology development

85 The research region is located in the Kuramenian Mountains (northern Tajikistan) near the
86 Fergana Basin (Fig. 1), where the climate is mainly affected by the Westerlies (Chen et al., 2016).
87 The average annual total rainfall from the closest meteorological station (Khujand station, 40.22 N,
88 69.73 E, 414 m a.s.l.) amounts to 164.1 mm, with only 19.1% of the total annual rainfall falling



89 during the warm season which is approximately from May to September. July (average monthly
90 temperature of 28.6 °C) and January (14.3 °C) are the warmest and the coldest month, respectively
91 (Fig. 2). At the sampling sites (Obiasht and Adrasman), with sparse vegetation among different
92 trees, open-canopy juniper forests grow on thin soil (Fig. 3). All tree-ring samples were collected
93 from the dominant species, Zeravshan juniper (*Juniperus seravschanica*), and in total, 81 samples
94 (from 40 trees) were taken from the two sites. The oldest tree (1594–2015) was found at the
95 Adrasman site.

96 After drying and mounted on the mounts, tree-ring samples were polished with the 400 grit
97 sandpapers to enhance tree-ring boundaries. The Velmex measuring system, with a precision of
98 0.001 mm, was used to measure annual ring widths. The quality of the cross-dating and
99 measurements was controlled using the COFECHA software (Grissino-Mayer, 2001). The result
100 of correlation analysis reveals that high correlation ($r= 0.52$, $p<0.001$) exists between the site
101 chronologies. This allowed us to use all tree-ring width series of juniper trees to construct a
102 regional chronology. The ARSTAN program (Cook and Kairiukstis, 1990) was used to develop a
103 regional chronology for the Kuramenian Mountains. Each raw ring-width series was first
104 detrended to remove non-climatic trends using the negative exponential curve. The standard (STD)
105 chronology was used in the further analyses. The fully replicated chronology with the expressed
106 population signal (Wigley et al., 1984) greater than or equal to 0.85 was achieved with a minimum
107 tree number of five trees from AD 1650.

108 2.2 Statistical analysis

109 The regional chronology was correlated with a set of monthly climate variables (including
110 monthly total rainfall and average temperature) from July of the previous year to September of



111 current year from the Khujand station for the period 1927–1990. Due to surrounding areas have
112 over a century of climate data, self-calibrating Palmer Drought Severity Index (scPDSI, Van der
113 Schrier et al., 2011) for the Kuramenian Mountains (averaged over 40.5–41.5 °N, 70.0–71.0 °E) for
114 the period 1901–2012 (obtained from the KNMI Climate Explorer website
115 (<http://climexp.knmi.nl/>) was also used in the correlation analysis.

116 Correlations between the regional chronology with the monthly climate records allowed
117 identification of the main limiting factors for tree growth. Based on linear regression analysis, a
118 statistical model between the predictand (scPDSI) and the predictors (the regional chronology)
119 was calculated for the calibration period (1901–2012) to indicate past drought variations. A
120 split-sample calibration-verification test (Cook and Kairiukstis, 1990) was used to evaluate the
121 reliability of the scPDSI reconstruction model. The period 1901–2012 was divided into calibration
122 (1957–2012) and verification (1901–1956) sections. The testing statistics were employed to
123 evaluate model ability, including sign test (ST), coefficient of efficiency (CE) and reduction of
124 error (RE) (Cook and Kairiukstis, 1990). Furthermore, to investigate common drought signals
125 among the existing moisture-sensitive tree-ring chronologies from Western Central Asia (this
126 study; Seim et al., 2015; Chen et al., 2016), principal component analyses (Jolliffe, 2002) was
127 used over the common period (1700–2012) of tree-ring chronologies from western Central Asia (.
128 In this study, wet and dry periods were determined if the 31-year low-pass values were lower than
129 the average value of the scPDSI reconstruction continuously for more than 10 years. We also
130 calculated the spatial correlation using the KNMI Climate Explorer (<http://climexp.knmi.nl/>) to
131 reveal the geographical representation of our records and also investigate correlation fields with
132 sea surface temperature (Rayner et al., 2003). Wavelet analysis was employed to reveal any



133 periodicities in the scPDSI reconstruction and the temporal stability of these (Torrence and Compo,
134 1998). For better visual comparison, the regional drought series of western and eastern Central
135 Asia were standardized and smoothed with a 20-year low-pass filter. In order to explore the
136 linkages between reconstructed scPDSI extreme events and atmospheric circulation patterns over
137 West and Central Asia, NCEP climate data (Kalnay et al., 1996) were used to create May-July
138 composite anomaly maps of the geopotential height, SSTs and 500-hPa vector wind in the driest
139 10 years and wettest 10 years during the period 1948–2010.

140 **3. Results**

141 3.1 The scPDSI reconstruction

142 Statistical results from the ARSTAN program indicated that over the common period
143 1901-2015, the Kuramenian Mountains chronology had a high standard deviation (0.45),
144 signal-to-noise ratio (32.22) and EPS (0.97). The Variance in first the eigenvector of all series
145 accounted for 51.6% of the total variance, indicating that juniper tree growth at the two sites was
146 influenced by similar factors. Significant positive correlations ($p < 0.05$) between the Kuramenian
147 Mountains chronology and monthly total precipitation were found in current April-July (r :
148 0.26–0.36) (Fig. 4). Significant negative correlations with monthly mean temperature were found
149 in current May-June (r : -0.28–0.44). The Kuramenian Mountains chronology was positively and
150 significantly correlated with scPDSI during previous July-September, particularly from April to
151 September (r : 0.59–0.637). We also investigated the correlations between the Kuramenian
152 Mountains chronology and seasonally averaged scPDSI, and the strongest correlation (r : 0.637)
153 was found with mean June-July scPDSI (1901–2012). The precipitation in June to September
154 accounts for 7.7% of the total annual precipitation, while June-July is the hottest months. The rise



155 in summer (June-July) temperatures promotes evaporation, and promotes the already existing
156 drought stress. Thus, the water availability in summer is the main limiting factor for the juniper
157 tree growth. Similar moisture influences on juniper growth have also been found in high Asia
158 (Zhang et al., 2015; Gou et al., 2015). Thus, the scPDSI reconstruction was developed by
159 calibrating the Kuramenian Mountains chronology with mean June-July scPDSI data.

160 During the calibration period 1901–2012, the predictor variable (the Kuramenian Mountains
161 chronology) accounts for 40.5% of the variance in the instrumental scPDSI data (40.0% after
162 adjustment for loss of degrees of freedom). The positive RE and CE reveal good predictive skill of
163 the statistical model (Table 2). The results of the sign and first-order sign tests both exceed the
164 99% confidence level. These test results indicated that our statistical equation was reliable. Figure
165 5 shows a comparison of reconstructed and instrumental mean June-July scPDSI data in the
166 Kuramenian Mountains during the period 1901–2012. The comparison shows that the
167 reconstructed scPDSI is quite consistent with the instrumental scPDSI on short and long
168 timescales during the 20th century.

169 3.2 Analyses of drought variation in the Kuramenian Mountains

170 The Kuramenian Mountains reconstruction provides insight into past drought variation for
171 this part of northern Tajikistan during the past four centuries (Fig. 6). Dry periods occurred in CE
172 1659–1696, 1705–1722, 1731–1741, 1758–1790, 1800–1842, 1860–1875 and 1931–1987.
173 Sustained dry decades were centered on 1830 as well as around 1960. Wet periods were identified
174 in CE 1742–1752, 1843–1859, 1876–1913, 1921–1930 and 1988–2015. Although the period
175 1988–2015 was characterized by wet summers, the reconstruction shows a downward trend during
176 the past 10 years, which is in agreement with the observations.



177 The three tree-ring width chronologies of juniper trees (this study; Seim et al., 2015; Chen et
178 al., 2016) were correlated significantly ($p < 0.001$) among each other. The principal component
179 analyses indicated that the first principal component (PC1) of the three chronologies exceed an
180 eigenvalue of >1.5 and account for 52.53% of the total variance. Spatial climate correlation
181 analyses revealed that the actual (Fig. 7a) and reconstructed (Fig. 7b) scPDSI series correlate
182 significantly with June–July gridded scPDSI and reveal similar spatial correlation fields, albeit the
183 signal strength of the latter is lower. Significant positive correlations were observed in the Fergana
184 Basin. The significant positive correlations of PC1 and June–July gridded scPDSI are also seen
185 from the Fergana Basin and the neighboring areas (Fig. 7c), suggesting similar large-scale drought
186 influence on Western Central Asia.

187 During the period 1901–2015, significant positive correlations ($p < 0.05$) for the
188 reconstructed scPDSI series of the Kuramenian Mountains with gridded SSTs over the tropical
189 oceans were found after removed the linear trends of SST data (Fig. 7d). Wavelet analysis
190 indicated that some centennial (100-150 years), decadal (50-60, 24.3 and 11.4 year) and
191 interannual (8.0, 2.0-3.5 years) periodicities were found in the reconstructed scPDSI data for the
192 Kuramenian Mountains (Fig. 8).

193 **4. Discussion**

194 4.1 Comparing reconstructed drought in western and eastern Central Asia

195 Based on two moisture sensitive tree-ring chronologies from central and western Tien Shan,
196 China (Chen et al., 2013; Chen et al., 2015b), Chen et al. (2015b) developed a regional scPDSI
197 reconstruction, accounting for 70.4% of the total variance in the observations, representing eastern
198 Central Asia. A comparison between the Kuramenian Mountains and the eastern Central Asia



199 reconstructions yielded a correlation coefficient of ($r > 0.35$, $p < 0.001$, $n=306$). The PC1 mirrors
200 similar dry/wet intervals as the drought series of eastern Central Asia (Fig. 8). Common dry
201 periods (1710s, 1770–1780s, 1800s, 1910–1940s and 1970–1980s) and wet periods (1720–1730s,
202 1790s, 1850s, 1890s, 1950–1960s and 1990–2000s) in western and eastern Central Asia suggest
203 similar moisture variation for both regions. Some differences, existing between the drought
204 records (i.e. in the 1700s, 1740–1760s, 1810–1840s, 1860–1880s and 1900s), may reflect local
205 influences in local geography (such as the eastern Central Asia is wetter) or the difference in tree
206 species (juniper and spruce). Despite of this, high correlation coefficient revealed that drought
207 stress is the major limiting factor on the tree growth of Central Asia, and covers the whole region.
208 Chen et al (2015b) also found significant correlations ($p < 0.05$) between the drought series of
209 eastern Central Asia with gridded SSTs over the tropical ocean, very similar to what was found for
210 the Turkestan juniper in this study, with a strong response to SSTs. Similar patterns suggesting
211 that the drought variations of eastern and western Central Asia may be linked with these tropical
212 domains. In particular, the eastern and western Central Asia both exhibit the wetting trend during
213 1970–2010s, implying that a consistent moisture increase in Central Asia which is of great
214 significance for alleviating the serious shortage of freshwater resources.

215 The driest year (1917) in the Kuramenian Mountains was also found in other regions of
216 Central Asia (Esper et al., 2001; Chen et al., 2013, 2015b, c; Seim et al. 2015). The second driest
217 year (1783) of the Kuramenian Mountains coincides with the volcanic eruption of Laki (iceland)
218 in 1783 (Schmidt et al., 2011; Chen et al., 2012), and suggests the influence of the volcanic
219 eruption on the climate there. In order to further reveal the characteristics of the large-scale
220 extreme drought events in Central Asia, we further extracted the first principal component of the



221 drought series of western and eastern Central Asia which accounted for 74.8% of the total
222 variance during the period 1901–2005. Based on this drought series, Large-scale drought events
223 during the period 1916-1919, 1944-1945 and 1974-1976 were found in Central Asia. Figure 10
224 showed that PDSI anomalies during the period 1916-1919, 1944-1945 and 1974-1976 are
225 noticeable negative over central and northern Asia, and the south Asia was anomalously wet. This
226 suggest the presence of weak moisture transport by south Asian monsoon and the Westerlies to
227 central Asia, and a weak south Asian monsoon with strong moisture transport in south Asia.

228 4.2 Possible climate drivers

229 The 24.3 and 11.4-year periodicity is likely related to the variations of large-scale modes of
230 solar activity (Hale, 1924; Hodell et al., 2001). In eastern Central Asia, the influence of solar
231 cycles on drought variations has been indicated by dendroclimatic researches (e.g., Li et al., 2006).
232 Thus, solar activity appears to have the large-scale impacts on the drought variations of Central
233 Asia. Comparison of the scPDSI reconstruction and the sunspot relative number series
234 (<http://www.sidc.be/silso/DATA/yearssn.dat>) also reveals there exists a significant relationship in
235 the 11 year band from the 1700–2000s (Fig. 9b). Similarly, the 8.0, 3.6 and 2.1-years cycles were
236 linked with the variations of the cross-equatorial low level jet of the western Indian Ocean (Gong
237 and Luterbacher, 2008) and El Niño -Southern Oscillation (ENSO) index (Li et al., 2013) (Fig. 9c,
238 9d). This suggests that drought variation in Central Asia may be related to large-scale
239 land–atmosphere–ocean circulation systems. However, some different relationships between the
240 series reveal that the impacts of solar activities (i.e. in the 1900–2000s) and large-scale climate
241 modes on the regional drought of the Central Asia are more complicated than expected, and a
242 number of unknown physical processes at various timescales await further investigation.



243 As previously mentioned, the drought variation of Central Asia may be teleconnected with
244 the activity of the south Asian summer monsoon. The wet-year composite is characterized by
245 strengthened southerlies and westerlies entered into Central Asia associated with a negative center
246 over Central Asia and some positive height-anomaly centers in the Near East and Indian ocean
247 (Fig. 11a, b). Positive SST anomalies were found in the tropical Indian and western Pacific Ocean
248 during the wettest years (Fig. 11e). Relatively abundant moisture is brought across the Arabian
249 Peninsula and Iranian Plateau by the strong southwesterly moisture flux (Asian summer monsoon)
250 and traveled further northward, causing increased moisture over the southern part of central Asia.
251 This finding resembles previous researches that have indicated drought variations over
252 southwestern and central Asia are strongly linked with the West Asian subtropical westerly jet and
253 SSTs in the tropical Indian oceans (Mariotti, 2007; Li et al., 2010; Zhao et al., 2014).

254 The composite of 500-hPa geopotential height during the driest years is the reverse of the
255 wettest-year composite in that the negative anomaly over Central Asia is replaced by a positive
256 anomaly (Fig. 11d). This positive anomaly combined with a relatively low over the Near East and
257 Indian Ocean suggests weakened southerlies over south Asia and perhaps an enhanced dry jet
258 across Central Asia (Fig. 11c). Previous researches has revealed that negative SST anomalies over
259 the tropical Indian Ocean tend to associate with weak southwesterly winds, and lead to increased
260 droughts in Central Asia (Vecchi et al., 2004; Li et al., 2010). This pattern during the driest years
261 supports such a connection. As seen above, moisture conditions in Central Asia are linked with
262 SSTs in the tropical oceans and Asian summer monsoon intensity. Dendroclimatic researches
263 based on the improved tree-ring network should help to understand the climate mechanisms of
264 Central Asia.



265 **5. Conclusions**

266 In this study, based on tree-ring width series of Turkestan juniper, we developed a new
267 June–July scPDSI reconstruction from the Kuramenian Mountains in northern Tajikistan, which
268 indicated drought variations at different time scales over the past 366 years. The drought
269 reconstruction captures the recent wetting trend of western Central Asia well, and represents
270 drought variations over a large area of western Central Asia. The dry/wet periods identified in the
271 drought reconstruction are in good agreement with drought series from eastern Central Asia.
272 Moreover, the analysis of links between the climate variations and our scPDSI reconstruction
273 reveals that there are some linkages of extremes in this scPDSI reconstruction with anomalous
274 Asian summer monsoon circulation in the Indian Ocean Rim. In Central Asia, Turkestan juniper
275 can live to about 500-1000 years (Esper et al., 2003). Thus, more efforts should be paid to extend
276 the dendroclimatic reconstructions by collecting the cores from the old trees and develop spatial
277 drought reconstructions to reveal the spatio-temporal drought variations of Central Asia.

278

279 **Acknowledgments**

280 This work was supported by NSFC Project (41405081) and National high level talents special
281 support plan. We thank the reviewers very much whose comments greatly benefitted this
282 manuscript.

283

284 **Contributions**

285 Conceived and designed the experiments: FC, ZT and KZ. Performed the experiments: FC, ZT,
286 AA and KA. Analyzed the data: FC and ZT. Contributed reagents/ materials/analysis tools: FC,



287 ZT, SA, and LH. Contributed to the writing of the manuscript: FC, SA, and LH.

288

289 **Conflict of Interest Statement**

290 The authors declare that the research was conducted in the absence of any commercial or financial
291 relationships that could be construed as a potential conflict of interest.

292

293 **Data Availability**

294 The authors confirm that all data underlying the findings are fully available without restriction.

295 The PDSI reconstruction is available in the Supplement.

296 **References**

297 Chen, F., Yuan, Y., Wei, W., Yu, S., Li, Y., Zhang, R., Zhang, T., and Shang, H.: Chronology
298 development and climate response analysis of Schrenk spruce (*Picea Schrenkiana*) tree-ring
299 parameters in the Urumqi river basin, China, *Geochronometria*, 36, 17-22, 2010.

300 Chen, F., Yuan, Y., Wei, W., Wang, L., Yu, S., Zhang, R., Fan, Z., Shang, H., Zhang, T., and Li, Y.:
301 Tree ring density-based summer temperature reconstruction for Zajsan Lake area, East Kazakhstan,
302 *Int. J. Climatol.*, 32, 1089-1097, 2012.

303 Chen, F., Yuan, Y.J., Chen, F.H., Wei, W.S., Yu, S.L., Chen, X.J., Fan, Z.A., Zhang, R.B., Zhang,
304 T.W., and Shang, H.M.: A 426-year drought history for Western Tian Shan, Central Asia, inferred
305 from tree rings and linkages to the North Atlantic and Indo-Pacific Oceans, *The Holocene*, 2013.
306 0959683613483614, 2013.

307 Chen, F., Yuan, Y.J., Wei, W.S., Zhang, T.W., Shang, H.M., and Zhang, R.: Precipitation
308 reconstruction for the southern Altay Mountains (China) from tree rings of Siberian spruce,
309 reveals recent wetting trend, *Dendrochronologia*, 32, 266-272, 2014.

310 Chen, F., Yuan, Y.J., Yu, S.L., Zhang, T.W., Shang, H.M., Zhang, R.B., Qin, L., and Fan, Z.A.: A
311 225-year long drought reconstruction for east Xinjiang based on Siberia larch (*Larix sibirica*)
312 tree-ring widths: Reveals the recent dry trend of the eastern end of Tien Shan, *Quaternary Int.*, 358,



- 313 42-47, 2015a.
- 314 Chen, F., Yuan, Y.J., Wei, W.S., Yu, S.L., Zhang, T.W., Shang, H.M., Zhang, R.B., Qin, L., and Fan,
315 Z.A.: Tree-ring recorded hydroclimatic change in Tianshan mountains during the past 500 years,
316 Quaternary Int., 358, 35-41, 2015b.
- 317 Chen, F., He, Q., Bakytbek, E., Yu, S.-l., and Zhang, R.-b.: Climatic signals in tree rings of
318 *Juniperus turkestanica* in the Gulcha River Basin (Kyrgyzstan), reveals the recent wetting trend of
319 high Asia, Dendrobiology, 74, 2015c.
- 320 Chen, F., Yu, S.L., He, Q., Zhang, R.B., Kobuliev, Z.V., and Mamadjonov, Y.M.: Comparison of
321 drought signals in tree-ring width records of juniper trees from Central and West Asia during the
322 last four centuries. Arab. J. Geosci., doi: 10.1007/s12517-015-2253-1, 2016.
- 323 Cook, E. R. and Kairiukstis, L. A.: Methods of dendrochronology: applications in the
324 environmental sciences, Kluwer Academic Publishers, Dordrecht, 394 pp., 1990.
- 325 Cook, E. R., Meko, D. M., Stahle, D. W., and Cleaveland, M. K.: Drought reconstructions for the
326 continental United States, J. Clim., 12, 1145-1162, 1999.
- 327 Cook, E.R., Seager, R., Kushnir, Y., Briffa, K.R., Büntgen, U., Frank, D., Krusic, P.J., Tegel, W.,
328 van der Schrier, G., Andreu-Hayles, L., Baillie, M., Baittinger, C., Bleicher, N., Bonde, N., Brown,
329 D., Carrer, M., Cooper, R., Čufar, K., Dittmar, C., Esper, J., Griggs, C., Gunnarson, B., Günther,
330 B., Gutierrez, E., Haneca, K., Helama, S., Herzig, F., Heussner, K.-U., Hofmann, J., Janda, P.,
331 Kontic, R., Köse, N., Kyncl, T., Levanič, T., Linderholm, H., Manning, S., Melvin, T.M., Miles, D.,
332 Neuwirth, B., Nicolussi, K., Nola, P., Panayotov, M., Popa, I., Rothe, A., Seftigen, K., Seim, A.,
333 Svarva, H., Svoboda, M., Thun, T., Timonen, M., Touchan, R., Trotsiuk, V., Trouet, V., Walder, F.,
334 Ważny, T., Wilson, R. and Zang, C.: Old World megadroughts and pluvials during the Common
335 Era, Sci Adv., 1, e1500561, 2015.
- 336 Dai, A.: Drought under global warming: a review, Wiley Interdisciplinary Reviews: Clim. Change,
337 2, 45-65, 2011.
- 338 Davi, N., Jacoby, G., Fang, K., Li, J., D'Arrigo, R., Baatarbileg, N., and Robinson, D.:
339 Reconstructed drought across Mongolia based on a large-scale tree-ring network: 1520–1993, J.
340 Geophys. Res., 115, D22103, 2010.
- 341 Easterling, D. R., Evans, J., Groisman, P. Y., Karl, T., Kunkel, K. E., and Ambenje, P.: Observed
342 variability and trends in extreme climate events: a brief review, Bull. Amer. Meteorol. Soc., 81,
15



- 343 417-425, 2000.
- 344 Esper, J., Treydte, K., Gärtner, H., and Neuwirth, B.: A tree ring reconstruction of climatic extreme
345 years since 1427 AD for Western Central Asia, *The Palaeobot*, 50, 141-152, 2001.
- 346 Esper, J., Schweingruber, F. H., and Winiger, M.: 1300 years of climatic history for Western
347 Central Asia inferred from tree-rings, *The Holocene*, 12, 267-277, 2002.
- 348 Esper, J., Shiyatov, S., Mazepa, V., Wilson, R., Graybill, D., and Funkhouser, G.:
349 Temperature-sensitive Tien Shan tree ring chronologies show multi-centennial growth trends,
350 *Clim. Dyn.*, 21, 699-706, 2003.
- 351 Fang, K., Davi, N., Gou, X., Chen, F., Cook, E., Li, J., and D'Arrigo, R.: Spatial drought
352 reconstructions for central High Asia based on tree rings, *Clim. Dyn.*, 35, 941-951, 2010.
- 353 Fritts, H. C. (Ed.): *Tree Rings and Climate*, Academic Press, London, 567 pp., 1976.
- 354 Gong, D.Y., and Luterbacher, J.: Variability of the low-level cross-equatorial jet of the western
355 Indian Ocean since 1660 as derived from coral proxies, *Geophys. Res. Lett.*, 35, L01705,
356 doi:10.1029/2007GL032409, 2008.
- 357 Gou, X., Gao, L., Deng, Y., Chen, F., Yang, M., and Still, C.: An 850-year tree-ring-based
358 reconstruction of drought history in the western Qilian Mountains of northwestern China,
359 *International Journal of Climatology*, 35, 3308-3319, 2015.
- 360 Hale, G. E.: The law of sun-spot polarity, *Proc. Natl. Acad. Sci. USA*, 10, 53, 1924.
- 361 Hodell, D. A., Brenner, M., Curtis, J. H., and Guilderson, T.: Solar forcing of drought frequency in
362 the Maya lowlands, *Science*, 292, 1367-1370, 2001.
- 363 Holmes, R. L.: Computer-assisted quality control in tree-ring dating and measurement, *Tree-ring*
364 *Bull.*, 43, 69-78, 1983.
- 365 Huang, J., Yu, H., Guan, X., Wang, G., and Guo, R.: Accelerated dryland expansion under climate
366 change, *Nature Climate Change*, 2015, doi: 10.1038/nclimate2837, 2015.
- 367 Kalnay, E., Kanamitsu, M., Kistler, R., Collins, W., Deaven, D., Gandin, L., Iredell, M., Saha, S.,
368 White, G., and Woollen, J.: The NCEP/NCAR 40-year reanalysis project, *Bull. Amer. Meteorol.*
369 *Soc.*, 77, 437-471, 1996.
- 370 Kezer, K., and Matsuyama, H.: (2006). Decrease of river runoff in the Lake Balkhash basin in
371 Central Asia. *Hydrol. Processes*, 20, 1407-1423, 2006.
- 372 Jolliffe, I.: *Principal component analysis*, Wiley Online Library, 2002.



- 373 Jones, P., Briffa, K., Osborn, T., Lough, J., Van Ommen, T., Vinther, B., Luterbacher, J., Wahl, E.,
374 Zwiers, F., and Mann, M.: High-resolution palaeoclimatology of the last millennium: a review of
375 current status and future prospects, *The Holocene*, 19, 3-49, 2009.
- 376 Li, J., Gou, X., Cook, E. R., and Chen, F.: Tree-ring based drought reconstruction for the central
377 Tien Shan area in northwest China, *J. Geophys. Res.*, 33, L07715, 2006.
- 378 Li, J., Cook, E., Chen, F., Gou, X., D'Arrigo, R., and Yuan, Y.: An extreme drought event in the
379 central Tien Shan area in the year 1945, *J. arid environ.*, 74, 1225-1231, 2010.
- 380 Li, J., Xie, S.P., Cook, E.R., Morales, M.S., Christie, D.A., Johnson, N.C., Chen, F.H., D'Arrigo,
381 R., Fowler, A.M., and Gou, X.: El Niño modulations over the past seven centuries, *Nature Climate*
382 *Change*, 3, 822-826, 2013.
- 383 Lioubimtseva, E. and Cole, R.: Uncertainties of climate change in arid environments of Central
384 Asia. *Reviews in Fisheries Science*, 14(1-2), 29-49, 2006.
- 385 Liu, Y., Lei, Y., Sun, B., Song, H., and Sun, J.: Annual precipitation in Liancheng, China, since
386 1777 AD derived from tree rings of Chinese pine (*Pinus tabulaeformis* Carr.), *Int. J. Biometeorol.*,
387 57, 927-934, 2013.
- 388 Mariotti, A.: How ENSO impacts precipitation in southwest central Asia, *Geophy. Res. Lett.*, 34,
389 doi: 10.1029/2007GL030078, 2007.
- 390 Micklin, P.P.: Desiccation of the Aral Sea: a water management disaster in the Soviet Union.
391 *Science*, 241(4870), 1170-1176, 1988.
- 392 Ososkova, T., Gorelkin, N., and Chub, V.: Water resources of central Asia and adaptation measures
393 for climate change, *Environ. Monit. Assess.*, 61, 161-166, 2000.
- 394 Palmer, W. C.: *Meteorological drought*, US Department of Commerce, Weather Bureau
395 Washington, DC, USA, 1965.
- 396 Rayner, N., Parker, D. E., Horton, E., Folland, C., Alexander, L., Rowell, D., Kent, E., and Kaplan,
397 A.: Global analyses of sea surface temperature, sea ice, and night marine air temperature since the
398 late nineteenth century, *Journal of Geophysical Research: Atmospheres*, 108, 2003.
- 399 Reyer, C. P., Otto, I. M., Adams, S., Albrecht, T., Baarsch, F., Carlsburg, M., Coumou, D., Eden,
400 A., Ludi, E., and Marcus, R.: Climate change impacts in Central Asia and their implications for
401 development, *Reg. Environ. Change*, 2015, doi: 10.1007/s10113-015-0893-z.
- 402 Schmidt, A., Ostro, B., Carslaw, K. S., Wilson, M., Thordarson, T., Mann, G. W., and Simmons, A.



- 403 J.: Excess mortality in Europe following a future Laki-style Icelandic eruption, *Proc. Natl. Acad.*
404 *Sci. USA*, 108, 15710-15715, 2011.
- 405 Schrier, G., Barichivich, J., Briffa, K., and Jones, P.: A scPDSI-based global data set of dry and wet
406 spells for 1901-2009, *J. Geophys. Res., Atmospheres*, 118, 4025-4048, 2013.
- 407 Seim, A., Tulyaganov, T., Omurova, G., Nikolyai, L., Botman, E., and Linderholm, H. W.:
408 Dendroclimatological potential of three juniper species from the Turkestan range, northwestern
409 Pamir-Alay Mountains, Uzbekistan, *Trees*, doi: 10.1007/s00468-015-1316-y, 2015.
- 410 Seftigen, K., Björklund, J., Cook, E.R. and Linderholm, H.W.: A tree-ring field reconstruction of
411 Fennoscandian summer hydroclimate variability for the last millennium. *Climate Dynamics* 44:
412 3141-3154, 2015.
- 413 Seim, A., Omurova, G., Azisov, E., Musuraliev, K., Aliev, K., Tulyaganov, T., Nikolyai, L.,
414 Botman, E., Helle, G., Dorado Liñan, I., Jivcov, S. and Linderholm, H.W.: Climate change
415 increases drought sensitivity of mountain juniper trees in Central Asia. *PlosOne* 11(4):e0153888.
416 DOI:10.1371/journal.pone.0153888, 2016.
- 417 Siegfried, T., Bernauer, T., Guiennet, R., Sellars, S., Robertson, A. W., Mankin, J., Bauer-Gottwein,
418 P., and Yakovlev, A.: Will climate change exacerbate water stress in Central Asia?, *Clim. Change*,
419 112, 881-899, 2012.
- 420 Solomina, O., Maximova, O., and Cook, E.: *Picea schrenkiana* ring width and density at the upper
421 and lower tree limits in the Tien Shan mts Kyrgyz republic as a source of paleoclimatic
422 information, *Geogr. Environ. Sustain.*, 1(7), 66-79, 2014.
- 423 Tian, Q., Gou, X., Zhang, Y., Peng, J., Wang, J., and Chen, T.: Tree-ring based drought
424 reconstruction (AD 1855-2001) for the Qilian Mountains, northwestern China, *Tree-ring Res.*, 63,
425 27-36, 2007.
- 426 Torrence, C. and Compo, G. P.: A practical guide to wavelet analysis, *Bull. Amer. Meteorol. Soc.*,
427 79, 61-78, 1998.
- 428 Touchan, R., Anchukaitis, K. J., Meko, D. M., Sabir, M., Attalah, S., and Aloui, A.: Spatiotemporal
429 drought variability in northwestern Africa over the last nine centuries, *Clim. Dyn.*, 37, 237-252,
430 2011.
- 431 Vecchi, G.A., Xie, S.P., Fischer, A.: Ocean-atmosphere covariability in the western Arabian Sea. *J.*
432 *Clim.*, 17, 1213-1224.



433 Vicente-Serrano, S. M., Beguer á, S., and López-Moreno, J. I.: A multiscalar drought index
434 sensitive to global warming: the standardized precipitation evapotranspiration index, *J. Clim.*, 23,
435 1696-1718, 2010.

436 Yao, J. and Chen, Y.: Trend analysis of temperature and precipitation in the Syr Darya Basin in
437 Central Asia, *Theor. Appl. Climatol.*, 120, 521-531, 2015.

438 Yuan, Y., Jin, L., Shao, X., He, Q., Li, Z., and Li, J.: Variations of the spring precipitation day
439 numbers reconstructed from tree rings in the Urumqi River drainage, Tianshan Mts. over the last
440 370 years, *Chin. Sci. Bull.*, 48, 1507-1510, 2003.

441 Zhang, T. W., Yuan, Y. J., Liu, Y., Wei, W. S., Yu, S. L., Chen, F., Fan, Z. A., Shang, H. M., Zhang,
442 R. B., and Qin, L.: A tree-ring based precipitation reconstruction for the Baluntai region on the
443 southern slope of the central Tien Shan Mountains, China, since AD 1464, *Quaternary Int.*, 283,
444 55-62, 2013.

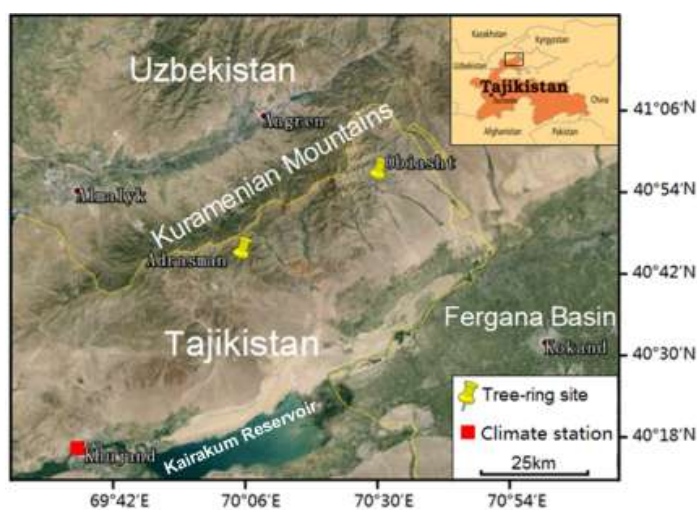
445 Zhang, Q.-B., Evans, M. N., and Lyu, L.: Moisture dipole over the Tibetan Plateau during the past
446 five and a half centuries, *Nat. commun.*, 6, 8062, 2015.

447 Zhao, Y., Wang, M., Huang, A., Li, H., Huo, W., and Yang, Q.: Relationships between the West
448 Asian subtropical westerly jet and summer precipitation in northern Xinjiang, *Theor. Appl.*
449 *Climatol.*, 116, 403-411, 2014.

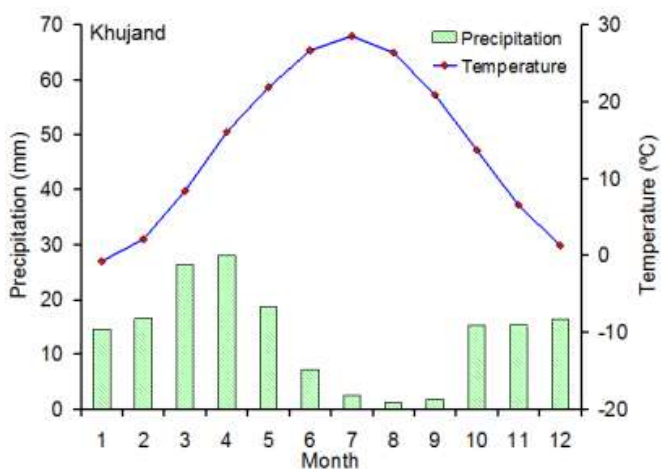
450
451
452
453
454
455
456
457
458
459
460
461
462



463
464
465
466
467
468
469
470



471
472 Fig. 1. Map of the climate station (Khujand) and the sampling sites in the Kuramenian Mountains,
473 northern Tajikistan.
474



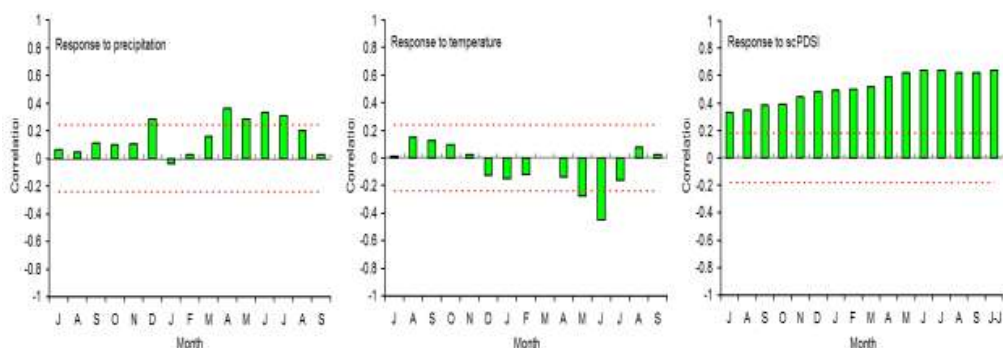
475

476 Fig. 2. Climate diagrams for the climate station of Khujand in northern Tajikistan.



477

478 Fig. 3. Juniper trees at the different sites in the Kuramenian Mountains, northern Tajikistan.



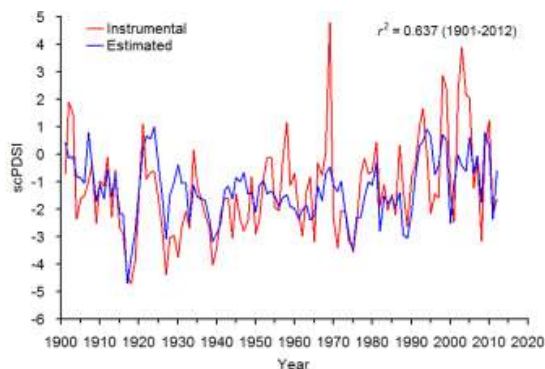
479

480

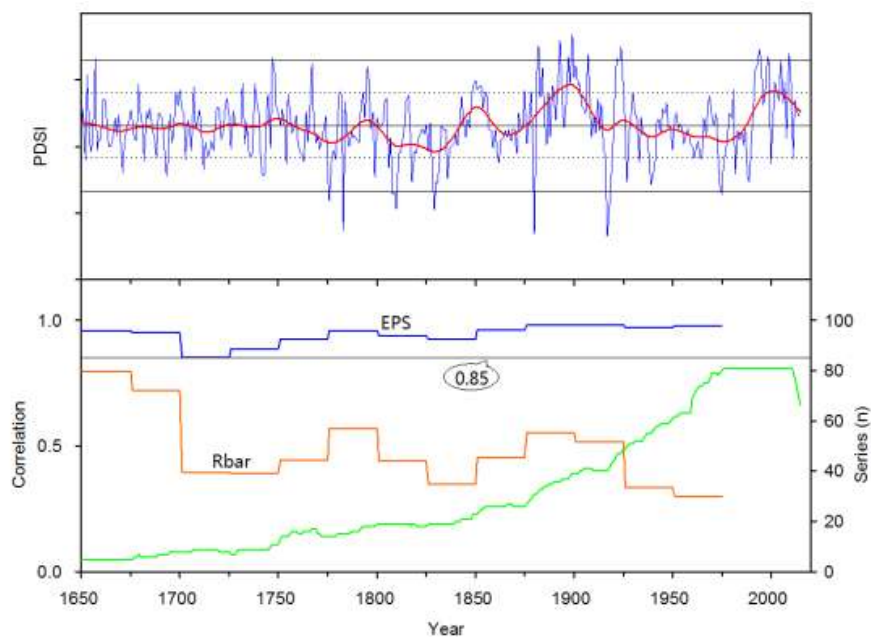
481 Fig. 4. Response plots for the regional chronology with monthly total precipitation (1927–1990),
 482 mean monthly temperature (1927–1990) and monthly scPDSI (1901–2012). The coefficients were



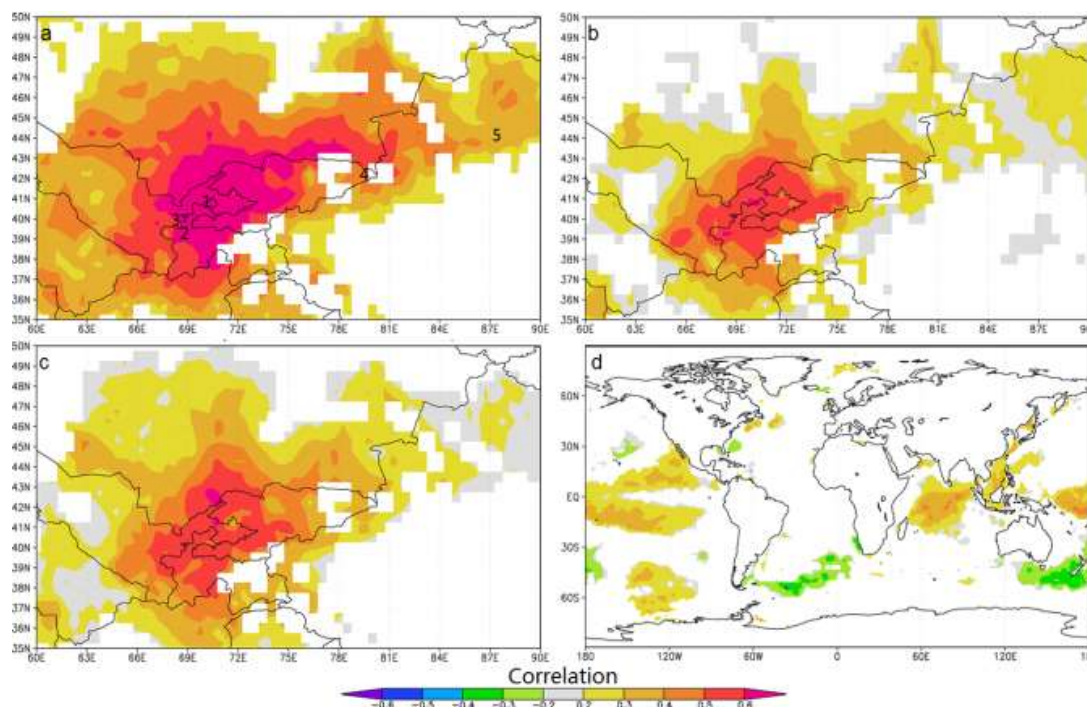
483 calculated from the previous July to the current September. Horizontal dashed lines denote 95%
 484 significance levels.



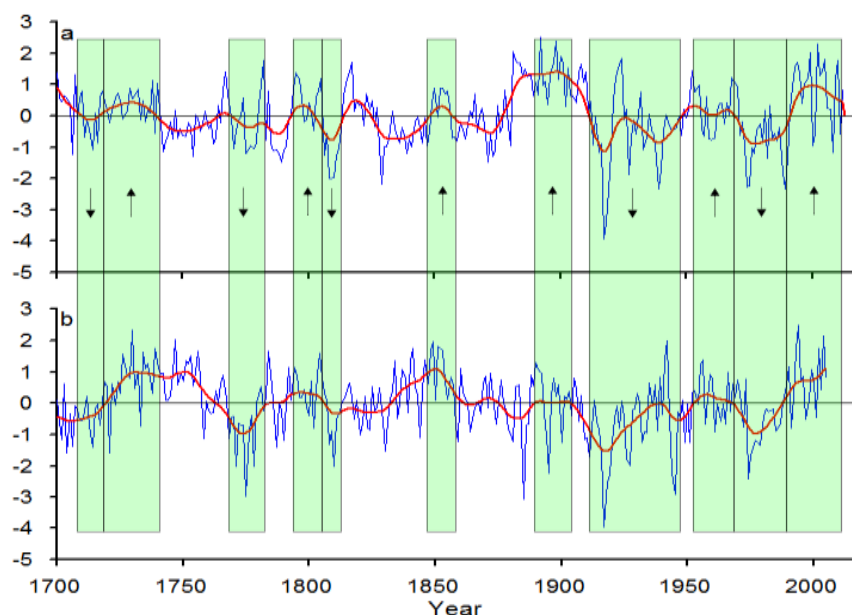
485
 486 Fig. 5. Comparison between the instrumental and reconstructed mean June–July scPDSI for the
 487 Kuramenian Mountains during the period 1901–2012.



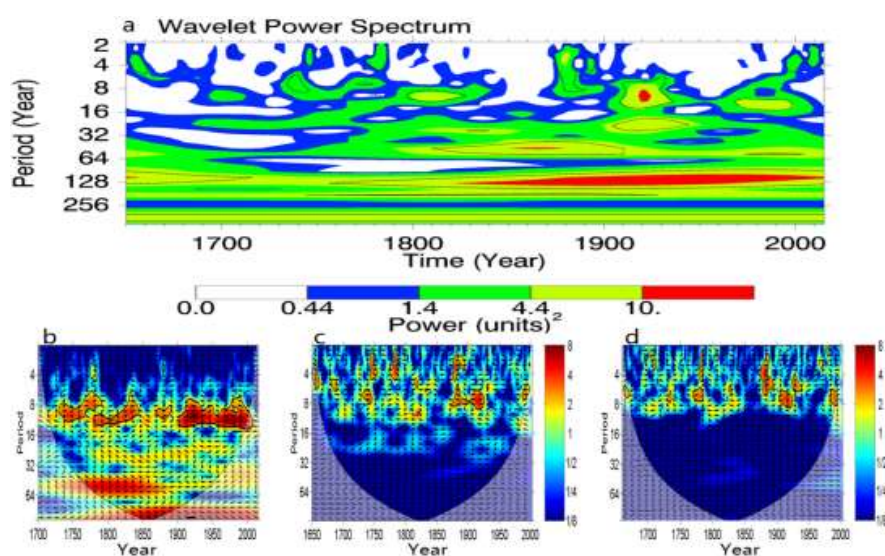
488
 489 Fig. 6. Reconstructed (thin line) and 31-year low-pass filter (thick line) values of June–July
 490 scPDSI for the Kuramenian Mountains from the regional chronology of the Kuramenian
 491 Mountains with sample size, EPS (expressed population signal) and Rbar (average correlation
 492 between series). Central horizontal line shows the mean of the estimated values; inner horizontal
 493 lines (dotted lines) show the border of one standard deviation, and outer horizontal lines two
 494 standard deviations. Rbar and EPS used moving 50-year windows, lagged 25 years.



495
496 Fig. 7. Spatial correlation fields of instrumental June–July scPDSI (a), reconstructed June–July
497 scPDSI (b) and PC1 (c) with regional gridded June–July scPDSI for the period 1901–2012. The
498 numbers 1, 2, 3, 4 and 5 denote the tree ring sites of northern Tajikistan (this study), western
499 Tajikistan (Chen et al., 2016), Uzbekistan (Seim et al., 2015), Kyrgyzstan (Chen et al., 2013), and
500 China (Chen et al., 2015b). (d) Spatial Pearson correlation plots for the reconstructed June–July
501 scPDSI for the Kuramenian Mountains with February–July averaged HadISST1 SST after
502 removed the linear trends of SST data during the period 1901–2015.
503



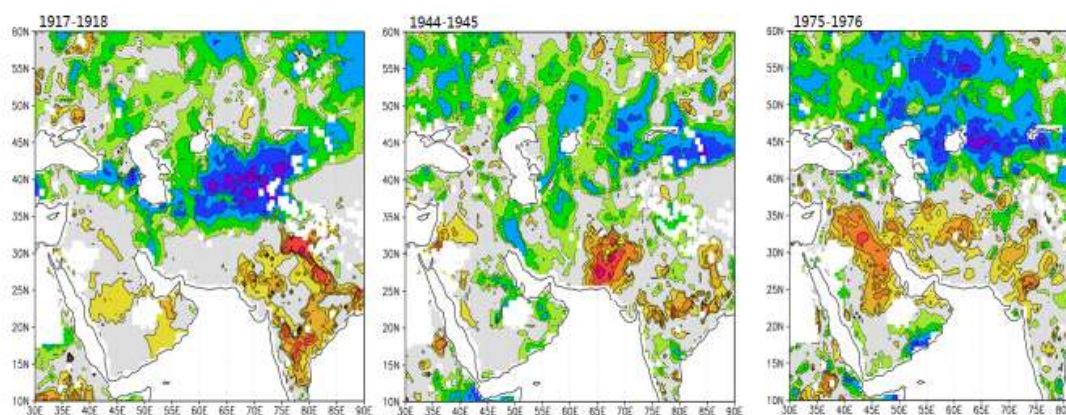
504
 505 Fig. 8. Comparison of between the drought series of western (a) and eastern Central Asia (b, Chen
 506 et al., 2015). All series were adjusted for their long-term means over the period 1700–2010, and
 507 smoothed with a 20-year low-pass filter to emphasize long-term fluctuations. The arrows indicate
 508 the upward/downward trends.



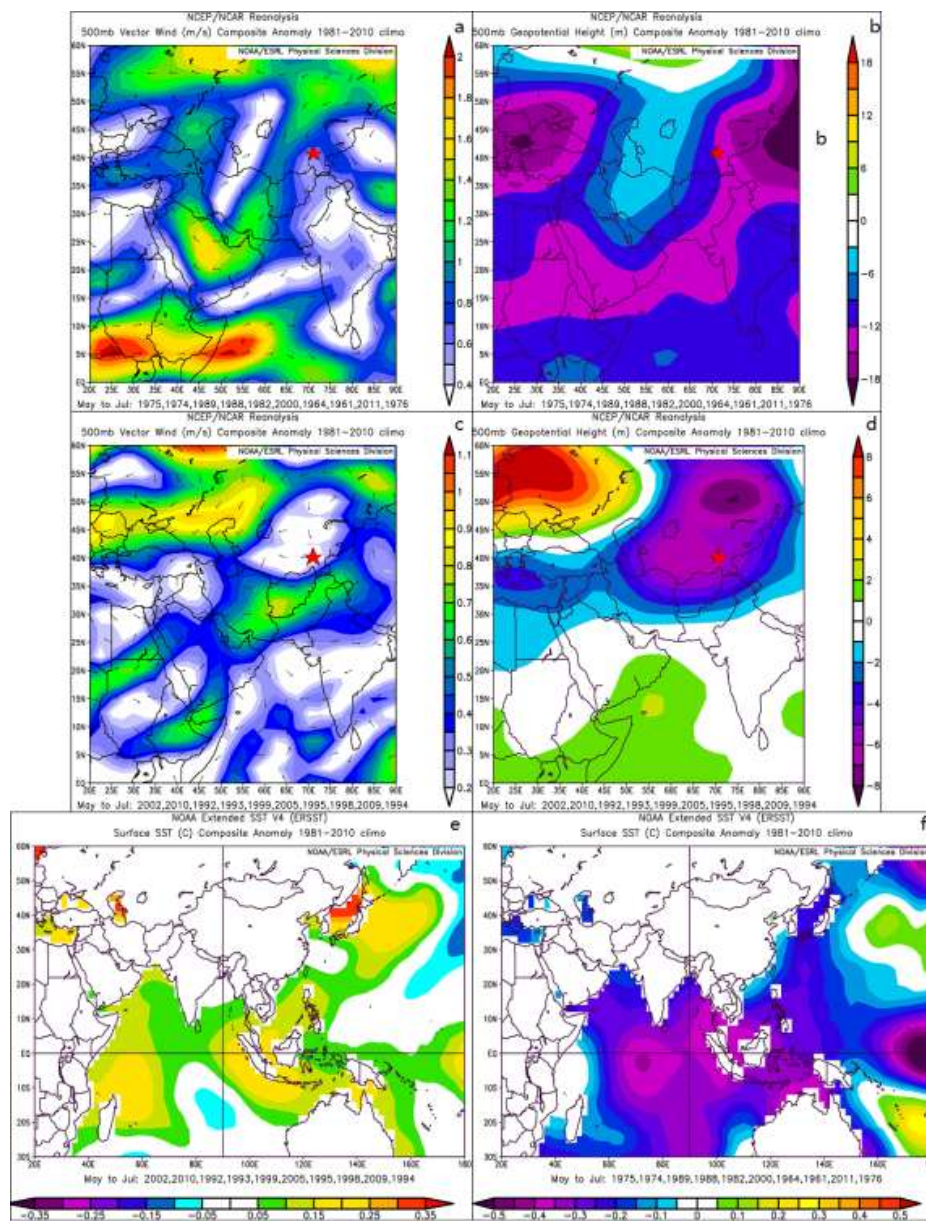
509
 510 Fig. 9. (a) The wavelet power spectrum. Black contours are the 5% significant level, using a
 511 red-noise (autoregressive lag 1) background spectrum. Cross wavelet transform of the
 24



512 reconstructed scPDSI of the Kuramenian Mountains with (b) sunspot number
513 (<http://www.sidc.be/silso/DATA/yearssn.dat>), (c) the ENSO index (Li et al., 2013) and (d) the
514 low-level cross-equatorial jet of the western Indian Ocean (Gong and Luterbacher, 2008). The 5%
515 significance level against red noise is shown as a thick contour. The relative phase relationship is
516 shown as arrows (with in-phase pointing to right, anti-phase pointing to left).



517
518 Fig. 10. PDSI anomalies during the dry period 1916-1919, 1944-1945 and 1974-1976.



519
 520 Fig. 11. Composite anomaly maps of the SSTs, 500-hPa vector wind and geopotential
 521 (from May to August) for the 10 wettest (a, b and e) and 10 driest (c, d and f) years for the scPDSI
 522 reconstruction during the period 1948–2010. The five-pointed star represent the study area.

523
 524



525 Table 1 Information about the sampling sites in the Kuramenian Mountains

Site code	Latitude (N)	Longitude (E)	Tree number	Elevation (m)	Aspect	Slope	Species
Obiasht	40°52'	70°27'	24	1663.7	E	30°	<i>J. seravschanica</i>
Adrasman	40°42'	70°04'	27	2035	SE	20°	<i>J. seravschanica</i>

526

527 Table 2 Calibration and verification statistics for mean June-July scPDSI reconstructions. *r*:
 528 correlation coefficient, RE: reduction of error, CE: coefficient of efficiency, ST: prediction sign
 529 test, FST: the first-order sign test prediction sign test '+': pair of actual and predicted temperatures
 530 showed same sign of departures from their respective mean values; '-': different sign of
 531 departures, *Significant at the 1% level.

	Calibration (1957-2012)	Verification (1901-1956)	Calibration (1901-1956)	Verification (1957-2012)	Full calibration (1901-2012)
<i>r</i>	0.705	0.637	0.637	0.705	0.637
<i>r</i> ²	0.410	0.406	0.406	0.410	0.406
RE		0.351		0.360	
CE		0.282		0.329	
Sign test		41+/15-*		41+/15-*	
First-order sign test		45+/10-*		46+/9-*	

532

533